JVI Journals.ASM.org

# Dynamics of Memory B-Cell Populations in Blood, Lymph Nodes, and Bone Marrow during Antiretroviral Therapy and Envelope Boosting in Simian Immunodeficiency Virus SIVmac251-Infected Rhesus Macaques

**Thorsten Demberg,[a] Egidio Brocca-Cofano,[a] Peng Xiao,[a] David Venzon,[b] Diego Vargas-Inchaustegui,[a] Eun Mi Lee,[c] Irene Kalisz,[c] V. S. Kalyanaraman,[c] Janet DiPasquale,[a] Katherine McKinnon,[a] and Marjorie Robert-Guroff[a]**

Vaccine Branch, National Cancer Institute, Bethesda, Maryland, USA[a]; Biostatistics and Data Management Section, National Cancer Institute, Bethesda, Maryland, USA[b]; and Advanced BioScience Laboratories, Inc., Rockville, Maryland, USA[c]

**Human immunodeficiency virus (HIV)/simian immunodeficiency virus (SIV) infection causes B-cell dysregulation and the loss of memory B cells in peripheral blood mononuclear cells (PBMC). These effects are not completely reversed by antiretroviral treatment (ART). To further elucidate B-cell changes during chronic SIV infection and treatment, we investigated memory B-cell subpopulations and plasma cells/plasmablasts (PC/PB) in blood, bone marrow, and lymph nodes of rhesus macaques during ART and upon release from ART. Macaques previously immunized with SIV recombinants and the gp120 protein were included to assess the effects of prior vaccination. ART was administered for 11 weeks, with or without gp120 boosting at week 9. Naïve and resting, activated, and tissue-like memory B cells and PC/PB were evaluated by flow cytometry. Antibody-secreting cells (ASC) and serum antibody titers were assessed. No lasting changes in B-cell memory subpopulations occurred in bone marrow and lymph nodes, but significant decreases in numbers of activated memory B cells and increases in numbers of tissue-like memory B cells persisted in PBMC. Macaque PC/PB were found to be either $CD27^+$ or $CD27^-$ and therefore were defined as $CD19^+$ $CD38^{hi}$ $CD138^+$. The numbers of these PC/PB were transiently increased in both PBMC and bone marrow following gp120 boosting of the unvaccinated and vaccinated macaque groups. Similarly, ASC numbers in PBMC and bone marrow of the two macaque groups also transiently increased following envelope boosting. Nevertheless, serum binding titers against SIVgp120 remained unchanged. Thus, even during chronic SIV infection, B cells respond to antigen, but long-term memory does not develop, perhaps due to germinal center destruction. Earlier and/or prolonged treatment to allow the generation of virus-specific long-term memory B cells should benefit ART/therapeutic vaccination regimens.**

Early and persistent B-cell dysfunction is a hallmark of human immunodeficiency virus (HIV) infection in humans (11, 20, 53) and precedes the loss of $CD4^+$ T cells, as shown in the simian immunodeficiency virus (SIV) rhesus macaque model (28). B-cell subpopulations and the expression of cluster-of-differentiation (CD) markers change during early HIV (22, 55) and SIV (28, 46, 58) infections. Patients on highly active antiretroviral therapy (HAART) who control viremia still exhibit B-cell dysregulation, e.g., activation, apoptosis, and abnormal CD marker expression, together with a skewing of B-cell populations, including the continued loss of memory populations and a lower frequency of naïve B cells (4, 15, 40, 48). The early initiation of HAART might be crucial for the preservation of B-cell functionality (37), as HAART treatment has been shown to partially reverse some of these B-cell defects (43, 57).

Multiple studies have examined virus-specific immune responses in patients or nonhuman primates treated with antiretroviral treatment (ART) or undergoing therapeutic vaccination with or without ART. To mention a few, investigations with humans have included the effects of vaccination with the canarypox ALVAC-HIV recombinant vaccine plus gp160 (25) and gp160 alone (19, 29), whereas in animals, therapeutic approaches have included vaccination with adenovirus type 5 (Ad5) and Ad35 recombinants (54), DNA vaccines plus interleukin-12 (IL-12) or IL-15 (21), and DNA encoding SIV Gag and rhesus cytomegalovirus (RhCMV) pp65 (24). However, these therapeutic approaches have focused either on $CD4^+$ T-cell recovery or on $CD8^+$ T-cell responses and their impact on viral loads. In a few cases, antibody responses have been assessed (25, 54); however, to our knowledge, no study of humans or nonhuman primates has addressed the longitudinal alterations of B-cell memory subpopulations during ART or during ART combined with therapeutic boosting.

Here we describe the results of our investigations of B-cell population dynamics in chronically SIV-infected rhesus macaques, either unvaccinated or previously vaccinated with ALVAC-SIV recombinants followed by SIV gp120 boosts, undergoing ART. In addition to ART alone, we evaluated the effects of the administration of an envelope protein boost shortly before release from ART. The goals of our study were to elucidate changes in B-cell memory subpopulations in blood, bone marrow (BM), and lymph node compartments over the course of ART and therapeutic vaccination. B-cell subpopulations are produced in the bone marrow, where B-cell precursors differentiate into immature B lympho-

**Received** 3 February 2012 **Accepted** 31 August 2012
**Published ahead of print** 12 September 2012
Address correspondence to Marjorie Robert-Guroff, guroffm@mail.nih.gov.
Copyright © 2012, American Society for Microbiology. All Rights Reserved.
doi:10.1128/JVI.00298-12

**TABLE 1** Treatment groups[a]

| Group | No. of macaques | Viral load (geometric mean copies/ml plasma) | Mean $CD4^+$ T-cell count (absolute counts/μl) ± SEM | Mean B-cell count (absolute counts/ μl) ± SEM | Treatment |
|---|---|---|---|---|---|
| Unvaccinated controls | 4 | $2.3 \times 10^5$ | 315 ± 96 | 624 ± 160 | ART (11 wk) |
| Unvaccinated boosted | 5 | $1.3 \times 10^6$ | 265 ± 89 | 426 ± 169 | ART (11 wk), gp120 boost at wk 9 |
| Vaccinated boosted | 5 | $7.6 \times 10^5$ | 271 ± 65 | 489 ± 141 | ART (11 wk), gp120 boost at wk 9 |

[a] Viral loads and $CD4^+$ T- and B-cell counts (means ± standard errors of the means) at the start of ART are listed. The control group originally had 5 macaques, with a geometric mean viral load of $3.0 \times 10^5$ copies/ml and $CD4^+$ and B-cell counts of 263 ± 91 and 527 ± 157, respectively. However, one macaque had to be sacrificed before the end of the experiment and was eliminated from the analyses.

cytes, and in lymphoid tissues, where memory B cells and plasmablasts (PB) mature in germinal centers following antigen exposure (reviewed in reference 45). Subsequently, these B-cell subpopulations recirculate in the peripheral blood to tissues, including the mucosa, and also to bone marrow, where long-lived plasma cells maintain antibody production. We reasoned that the monitoring of these three compartments would provide a comprehensive picture of B-cell population dynamics. We anticipated that envelope boosting would be reflected by increases in B-cell memory and SIV Env-specific plasma cell (PC)/PB counts and even more so in previously vaccinated macaques. The latter situation will become more relevant for human populations as more individuals participate in vaccine trials which are only partially protective. We hoped to shed light on whether the boosting of previously vaccinated individuals would be of benefit in terms of enhanced B-cell memory and the maintenance of reduced viremia following the cessation of ART. Moreover, early ART treatment has been shown to prevent HIV transmission (7) and will be implemented extensively in order to control the AIDS epidemic. Thus, an understanding of the effects of ART on subpopulations of immune cells, including B cells, will facilitate the design of improved therapeutic regimens.

## MATERIALS AND METHODS

**Animals and antiretroviral treatment.** Fourteen chronically SIV-infected outbred male rhesus macaques (*Macaca mulatta*) were obtained from two previous vaccine studies (64; P. Pegu et al., unpublished data) and housed according to NIH guidelines for animal use at Advanced Bioscience Laboratories, Inc. (ABL, Rockville, MD). The animals were divided into 3 groups according to their prior vaccination status and the planned therapeutic regimen (unvaccinated controls, unvaccinated boosted, and vaccinated boosted) and balanced to achieve similar viral loads and $CD4^+$ T-cell counts across the 3 groups (Table 1). All animals had been previously infected intrarectally by repeated low-dose challenges with a 1:500 dilution of a SIVmac251 stock equivalent to 125 50% tissue culture infective doses ($TCID_{50}$). At the time of the initiation of the study, 10 of the macaques had been infected for 27 to 32 weeks and 4 had been infected for 60 to 65 weeks.

All animals were treated with antiretroviral therapy (ART) for 11 weeks, as follows: intravenous didanosine (ddI; Videx), at 10 mg/kg of body weight/day for the first 3 weeks and then 5 mg/kg/day; oral stavudine, at 1.2 mg/kg/dose twice per day; and subcutaneous 9-(2-phosphonylmethoxypropyl) adenine (PMPA), at 20 mg/kg/day. At week 9, animals in group 2 (unvaccinated) and group 3 (previously vaccinated with gp120) received 100 μg of SIV gp120 adjuvanted with monophosphoryl lipid A-stable emulsion (MPL-SE) intramuscularly. Blood and bone marrow samples were obtained at weeks 0, 8, 11, 13, and 19. Lymph nodes were obtained at weeks 0, 8, and 13. Cells were isolated as previously described (10) and analyzed as described below.

Viral loads in blood and tissue were determined by nucleic acid sequence-based amplification (NASBA) (32, 49). Absolute $CD4^+$ T-cell and B-cell counts were obtained by using whole blood and Trucount tubes (BD Bioscience, San Jose, CA).

**Antibody binding and antibody-secreting cells.** Serum binding titers against SIV gp120 were measured as follows: wells of Nunc Maxisorb 96-well plates were coated overnight at 4°C with 50 ng/well of gp120 in 100 μl of sodium bicarbonate buffer (pH 9.6) (Sigma-Aldrich, St. Louis, MO). Wells were blocked with 200 μl of SuperBlock blocking buffer (Pierce) in phosphate-buffered saline (PBS) for 1 h at room temperature (RT). Serially diluted serum samples (100 μl) were added and incubated for 1 h at 37°C. Plates were washed 5 times with PBS containing 0.05% Tween 20 (Sigma-Aldrich). Horseradish peroxidase-labeled goat anti-human IgG (100 μl at a 1:100,000 dilution; Rockland, Gilbertsville, PA) was added, and plates were incubated for 1 h at 37°C. After washing as described above, 100 μl of K-Blue aqueous 3,3′,5,5′-tetramethylbenzidine (TMB) substrate (Neogen) was added for 30 min at RT. Color development was stopped with 2 N sulfuric acid (Fisher), and plates were read at 450 nm by using a Molecular Devices E-max plate reader. The antibody titer was defined as the reciprocal of the serum dilution at which the absorbance of the test serum was twice the absorbance of a negative macaque serum sample at a 1:50 dilution.

B-cell enzyme-linked immunosorbent spot (ELISpot) assays were performed on bone marrow-derived cells and peripheral blood mononuclear cells (PBMC), as previously described (3). Numbers of antibody-secreting cells (ASC) are reported as averages of data from triplicate determinations.

**Flow cytometry.** B-cell populations in bone marrow, axillary lymph nodes, and PBMC were analyzed by flow cytometry. Briefly, $2 \times 10^6$ cells were stained with viability dye (Aqua; Life Technologies, Carlsbad, CA) for 10 min at RT in the dark. The cells were then washed with Dulbecco's phosphate buffered saline (DPBS) (Lonza) and stained for 25 min at RT in the dark with a cocktail of antibodies (Table 2), with appropriate fluorescence-minus-one (FMO) and isotype controls. After washing with DPBS, the cells were fixed in 2% formaldehyde solution (Touisimis, Rockville,

**TABLE 2** Antibodies used for flow cytometry

| Antigen | Clone | Color | Supplier |
|---|---|---|---|
| CD3 | SP34-2 | Pacific blue | BD Bioscience |
| CD14 | Tuk4 | Qdot605 | Invitrogen |
| CD19 | J3-119 | PE-Cy5 | Beckman Coulter |
| CD20 | 2H7 | eF650NC | eBioscience |
| CD21 | B-ly4 | PE-Cy7 | BD Bioscience |
| CD22 | RBI4 | APC | Invitrogen |
| CD27 | O323 | APC-Cy7 | eBioscience |
| CD38 | AT-1 | FITC | StemCell Technologies |
| CD138 | DL-101 | PE | eBioscience |
| CD279 | eBioJ105 | PerCP-eF710 | eBioscience |
| Viability dye | NA[a] | Aqua | Invitrogen |

[a] NA, not applicable; APC, allophycocyanin; FITC, fluorescein isothiocyanate; PerCP, peridinin chlorophyll protein.

MD) and acquired the same day on a custom four-laser BD LSR-II instrument (BD Bioscience). A minimum of 250,000 live $CD3^-$ $CD14^-$ cells were acquired with FACSDIVA 6.1.3. Populations were analyzed by using FlowJo 9.3.1. The data were exported, and graphs were generated with GraphPad Prism 5.04.

**B-cell sorting and analysis.** Cryopreserved bone marrow cells from 4 randomly selected, chronically infected rhesus macaques were thawed, counted, and stained with viability dye as described above. The cells were washed with PBS and stained for 25 min in the dark at RT with the following antibody cocktail: CD3 phycoerythrin (PE) or CD3 Pacific blue (SP34-2), CD14 Qdot605 (Tuk4), CD21 PE-Cy7 (b-ly4), CD27 Ax700 (O323), and CD19 PE-Cy5 (J3-119). Cells were washed and kept on ice in sort buffer (Hanks balanced salt solution [HBSS] with 15 mM HEPES, 1% bovine serum albumin [BSA], penicillin-streptomycin, and 2 mM EDTA) until sorting was done with a FACSAria instrument. Viable sorted $CD3^-$ $CD14^-$ $CD19^+$ $CD21^-$ $CD27^-$ B cells were washed in R10 medium, and 10,000 cells were seeded in triplicate into wells of 96-well MultiScreen HTS plates coated with anti-rhesus macaque IgG or IgA antibody. Following overnight incubation, B-cell ELISpots were developed and counted, as previously described (3). $CEM.NK^R$ cells (AIDS Research and Reference Reagent Program, DAIDS, NIAID, NIH) (23) served as negative controls.

**Statistical analyses.** Total $CD4^+$ T-cell and B-cell counts were analyzed by the Wilcoxon signed-rank test and linear regression analysis, following square root transformation of the $CD4^+$ T-cell counts and log transformation of the B-cell counts. Analysis of the memory B-cell subpopulations in bone marrow and PBMC was accomplished by using a repeated-measures analysis of variance (ANOVA) of arc-sine-transformed percentages. Analysis of the lymph node subpopulations was done according to the same method, except that the activated and tissue-like subpopulations were log transformed prior to analysis. A repeated-measures ANOVA was similarly used to analyze PC/PB counts, ASC counts, binding titers, and PD-1 expression following log transformation of the data. CD22 data were arc-sine transformed prior to analysis by repeated-measures linear regression.

## RESULTS

**Viral loads and $CD4^+$ T-cell and B-cell counts.** After the initiation of ART, viral loads were reduced approximately 2 logs within 2 weeks in all groups (Fig. 1A). Thereafter, the suppression of viremia remained suboptimal, with only control macaques exhibiting a further decline over the 11 weeks of treatment, most likely reflecting the variability in the response to treatment among the macaques. Two macaques in the unvaccinated boosted group developed elevated amylase and lipase levels at week 9, so their ddI was stopped, with no significant effect on the geometric mean viral load of the group. All other therapies were continued per the protocol. The unvaccinated and vaccinated macaques were boosted with SIVmac251 gp120 on week 9, with no effect on viral loads. Upon the cessation of ART, viral rebound was observed; however, viremia levels in each group subsequently remained at the levels observed over an 11-week period prior to the initiation of ART.

$CD4^+$ T-cell counts exhibited no differences between groups over the course of the study. However, during ART (weeks 0 to 11), $CD4^+$ T-cell counts increased, as seen previously (59), from an overall mean of 282 cells/μl in all groups to 605, 690, and 630 cells/μl in the control, unvaccinated, and vaccinated groups, respectively (Fig. 1B). Following square root transformation, linear regression analysis of the counts obtained from each macaque over the 11 weeks produced positive slopes in all cases ($P < 0.0001$ by signed-rank analysis). As expected, $CD4^+$ T-cell counts immediately started to decline after release from ART. By week 19, no difference in $CD4^+$ T-cell counts remained for the three groups compared to the week 0 values.

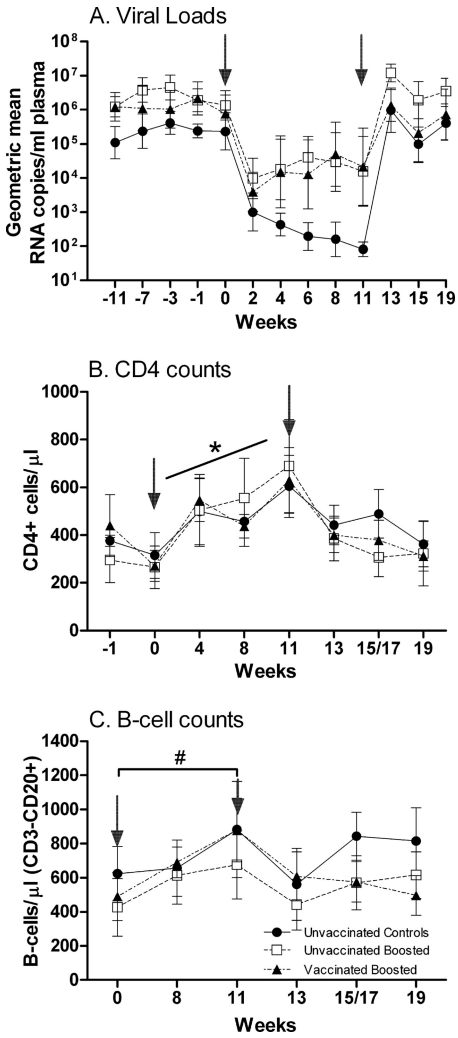


**FIG 1** Viral loads and absolute CD4 and B-cell counts over the duration of the study. (A) Geometric mean plasma viremia. Standard error bars are shown. (B) Absolute CD4 counts (means ± standard errors of the means) in PBMC. *, positive slope for each macaque over weeks 0 to 11 ($P < 0.0001$). (C) Absolute B-cell counts (mean $CD20^+$ counts ± standard errors of the means) in PBMC. #, significant increases in B-cell counts between weeks 0 and 11 ($P = 0.011$). Arrows indicate times of ART (0 to 11 weeks).

Similar to the $CD4^+$ T-cell counts, absolute B-cell numbers in PBMC were not different between groups over the course of the study (Fig. 1C). Following log transformation, a significant increase in B-cell counts between weeks 0 and 11 was observed by the Wilcoxon signed-rank test ($P = 0.011$) as well as by linear regression, confirming a previous report of increased B-cell counts during ART (28). This increase can be attributed to ART alone rather than envelope boosting, as no difference was observed between the control macaques and the boosted unvaccinated or vaccinated macaques. Taking all the macaques together, 10 had higher B-cell counts at week 19 than at week 0 ($P = 0.020$). The overall increase was small, however, amounting to a mean of 124 B cells/μl.

**B-cell gating and definition of memory B-cell subpopulations.** To evaluate memory B-cell subpopulations, the gating strategy used was slightly different for PBMC than for bone mar-

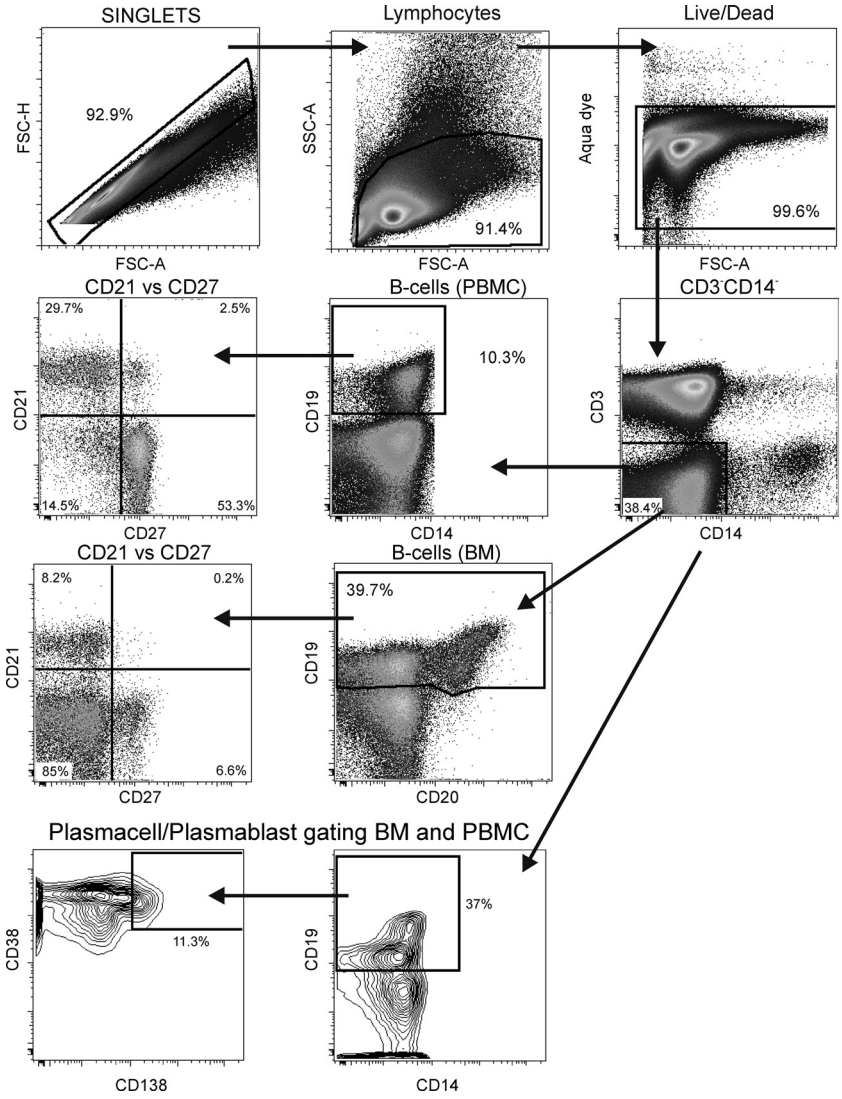


**FIG 2** Flow cytometry gating strategy. A representative gating of memory B cells in PBMC and bone marrow is shown. Singlets were gated on lymphocytes, followed by a live/dead gate and selection of $CD3^-$ $CD14^-$ cells. B cells in PBMC were identified by gating on $CD19^+$ cells, and B cells in bone marrow (BM) and lymph node were identified by a combination of CD19 and CD20. Naïve cells and resting, activated, and tissue-like memory cells were distinguished by CD21 versus CD27 gating. PC/PB were defined as $CD38^+$ $CD138^+$ for BM. FSC-H, forward scatter height; FSC-A, forward scatter area.

row and lymph node cells (Fig. 2). For PBMC, it was only necessary to gate on $CD19^+$ cells which also coexpressed CD20. In contrast, the majority of bone marrow B cells are $CD19^+$ $CD20^{+/-}$ (Fig. 2), and lymph node B cells (not shown) are $CD19^+$ $CD20^{+/dim}$. The use of both markers facilitated the identification of all B cells, and in lymph nodes, it made the identification of B cells more stringent. In defining memory B-cell subpopulations, we used the following nomenclature described previously by Titanji et al. (58) (Fig. 2): naïve ($CD21^+$ $CD27^-$), resting memory ($CD21^+$ $CD27^+$), activated memory ($CD21^-$ $CD27^+$), and tissue-like memory ($CD21^-$ $CD27^-$). Tissue-like memory B cells in HIV-infected humans were previously described to be similar to tonsillar tissue memory B cells ($CD20^{hi}$ $CD21^{lo}$ $CD27^-$) (39). Notably, we did not include the CD10 marker for immature B cells in our gating strategy (51). CD10 staining in HIV-infected individuals can be variable. Fogli et al. (18) reported previously that levels of $CD21^-$ $CD27^-$ tissue-like memory cells are elevated in HIV-infected patients and that these cells are essentially negative for CD10, representing an exhausted phenotype. Malaspina et al. (34) reported previously that the elevated $CD21^-$ $CD27^-$ cell population in HIV-positive individuals could be either $CD10^+$, representing immature cells, or $CD10^-$, representing exhausted tissue-like memory cells. Upon the testing of PBMC and bone marrow cells from either healthy or chronically infected rhesus macaques, we found very few $CD10^+$ cells using two different CD10 antibodies (clones HI10a and J5). Therefore, CD10 was excluded from the panel in favor of other markers.

**Dynamics of memory B-cell subpopulations during ART and therapeutic immunization.** Prior to ART, naïve B cells in bone marrow accounted for approximately 5 to 20% of all B cells (Fig. 3A to C). All three macaque groups received identical ART over the first 8 weeks of the study, and macaques of all groups taken together showed a significant increase in naïve B-cell counts over this time period ($P = 0.0005$) (Fig. 3A to C), suggesting that even

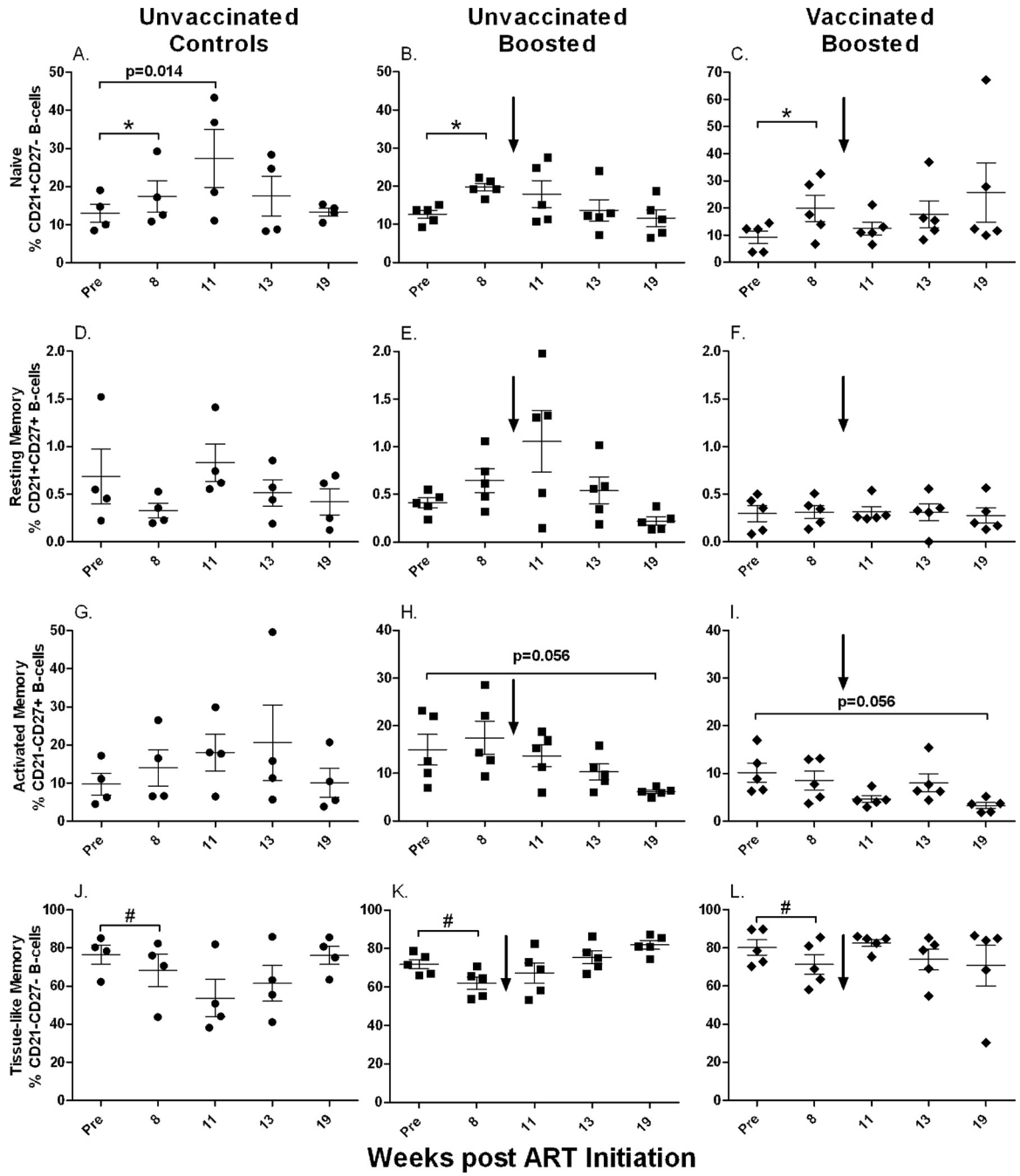


**FIG 3** Memory B cells in bone marrow over the course of the study. Shown are changes in naïve (A to C), resting memory (D to F), activated memory (G to I), and tissue-like memory (J to L) B cells over the duration of the study. *, significant increase in numbers of naïve B cells when all groups were combined ($P = 0.0005$); #, significant decrease in numbers of tissue-like memory B cells when all groups were combined ($P = 0.015$). Values for individual animals are plotted, with the group means (long solid lines) and standard errors of the means (short solid lines) shown. Arrows indicate boosting with SIV gp120 at week 9.

chronically infected macaques retain the ability to generate new naïve B cells. This increase was balanced by a significant decrease in numbers of tissue-like memory cells over the same time period for all three groups combined ($P = 0.015$) (Fig. 3J to L). Therapeutic boosting with gp120 did not affect the naïve B-cell population. The control group showed an increase in naïve B-cell numbers from the pre-ART time point to week 11 ($P = 0.014$) (Fig. 3A), but following the normalization of B-cell percentages at weeks 8 and 11 to pre-ART values, no differences were seen between the control and boosted groups, whether previously vaccinated or not (data not shown). Overall, the initial increase of naïve B-cell numbers under ART was not sustained, and levels at week 19 were not different from pre-ART values.

Resting memory B cells were the smallest population in bone marrow, consistently less than 2% (Fig. 3D to F). Over the course of the study, this population did not change during ART, nor did

boosting lead to significant changes. In contrast, throughout the study, the activated memory B-cell population showed no consistent changes in the control macaques (Fig. 3G) but tended to decline in the boosted groups (Fig. 3H and I). However, the differences between the pre-ART and week 19 values in the boosted groups were marginally nonsignificant ($P = 0.056$ for both).

Tissue-like memory B cells represented the largest population in bone marrow, making up 60 to 90% of all B cells prior to ART (Fig. 3J to L). However, note that, as discussed above, anti-CD10 antibody was not included in our staining panel. Therefore, some of the cells in this compartment could have been pro-B or immature B cells (51). Whether the expression level of CD10 declines in this bone marrow population, as in PBMC of HIV-infected individuals (18), will require further study. As mentioned above, during the first 8 weeks of ART, the numbers of tissue-like memory cells declined in all three macaque groups but thereafter returned to pre-ART levels. No difference was seen between pre-ART and week 19 values for any group.

In PBMC, the overall distribution of B-cell memory subpopulations was very similar to that in bone marrow. Naïve B cells represented a slightly larger fraction (Fig. 4A to C), but no increase during the first 8 weeks of ART was seen for any of the three groups. Furthermore, values at week 19 were not different from pre-ART levels. Unlike the population in bone marrow, however, numbers of resting memory cells in PBMC were increased after 11 weeks of ART (Fig. 4D to F). Geometric means of the fold increases in values from week 8 to 11 were 2.99 for the controls (Fig. 4D), 2.71 for the unvaccinated group (Fig. 4E), and 2.66 for the vaccinated group (Fig. 4F). Differences between the week 8 and week 11 values were statistically significant for all three groups, with equivalent $P$ values of $<0.0001$. As the extents of the increases were similar in all three groups, we conclude that the envelope protein boost had no impact on resting memory B-cell levels in PBMC. Furthermore, after release from ART, levels of resting memory cells in all groups declined to pre-ART levels, with no differences between groups (Fig. 4D to F).

While activated memory cells in bone marrow showed a tendency toward a decline in the unvaccinated and vaccinated groups over the course of treatment, clear changes were noted for the activated memory B-cell population in PBMC (Fig. 4G to I). Here activated memory cells were continuously lost, leading to significant decreases at week 19 compared to pre-ART values for control ($P = 0.0076$), unvaccinated ($P < 0.0001$), and vaccinated ($P = 0.0002$) macaques. The decline in numbers of activated memory B cells was countered by an increase in numbers of tissue-like memory B cells in all groups over the course of treatment. Significant differences between week 19 and pre-ART levels were obtained for the control ($P = 0.0068$), unvaccinated ($P < 0.0001$), and vaccinated ($P = 0.0068$) groups (Fig. 4J to L), suggesting a transition from an activated memory to a tissue-like memory phenotype.

The overall distribution of B-cell subpopulations in lymph node differed strongly from those in bone marrow and PBMC, which were more similar to each other. Naïve B cells made up the largest population in lymph node, consisting of approximately 65 to 98% of all B cells (Fig. 5A to C). Moreover, the resting memory population was on average 4 times larger (Fig. 5D to F) than that in BM and PBMC. In contrast, activated memory cells (Fig. 5G to I) represented the smallest population, perhaps indicating homing to other tissue sites. The tissue-like memory B-cell population was also smaller than its respective counterparts in blood and bone marrow (Fig. 5G to L). The numbers of resting memory B cells for all groups combined increased over the first 8 weeks of ART ($P = 0.0034$), while the numbers of tissue-like memory B cells declined during the same period ($P = 0.0029$). By week 13, however, after ART release, memory B-cell subpopulations were unchanged compared to pre-ART levels.

**Previously vaccinated animals respond to protein boosting at a magnitude similar to that for unvaccinated animals.** We next investigated changes in PC/PB populations. In humans, PC/PB are $CD20^{-/dim}$. Gating on both CD19 and CD20 helped identify them in macaques. PC/PB were initially sought in the four memory B-cell compartments of bone marrow using the additional markers $CD138^+$ (Syndecan-1) and $CD38^{hi}$. Although only about half of human PC/PB in the blood express CD138 at a low mean fluorescence intensity (MFI) (36), we found this to be a useful marker in macaques. Further distinction of PC and PB using markers such as Ki67 was not performed, as we were limited in the overall antibody panel. We were surprised to see $CD38^{hi}$ $CD138^+$ cells in the tissue-like memory compartment ($CD21^-$ $CD27^-$) in addition to positive cells in the activated memory ($CD21^-$ $CD27^+$) subpopulation (data not shown). In humans, PC/PB are characterized by the expression of CD27. Therefore, to confirm that the $CD21^-/CD27^-$ B cells were genuine PC/PB and spontaneously secreting antibody, we sorted this population of B cells from viably frozen bone marrow obtained from 4 of the study animals prior to the initiation of ART. The cells were thawed and stained as described in Materials and Methods. We obtained sorted populations of >95% purity (Fig. 6A). The sorted cells were plated onto anti-IgG or anti-IgA antibody-coated plates and incubated overnight without stimulation. We observed robust numbers of B cells spontaneously secreting IgG and IgA (Fig. 6B), confirming that rhesus macaque PC/PB can have a $CD27^-$ phenotype. Among the 4 macaques, the range of IgG ASC counts was 2,500 to 70,433 ASC/$10^6$ $CD21^-/CD27^-$ B cells. The IgA ASC counts ranged from 300 to 16,667 ASC/$10^6$ $CD21^-/CD27^-$ B cells (data not shown). No spots were observed by using $CEM.NK^R$ negative-control cells. Subsequently, macaque PC/PB were simply defined as $CD19^+$ $CD38^{hi}$ $CD138^+$ (Fig. 2) for further analyses.

In bone marrow, taking all the macaques together, a significant decrease in the number of PC/PB was observed during the first 8 weeks of ART ($P = 0.011$) (Fig. 7A). PC/PB expanded significantly following the boosting of both the vaccinated and unvaccinated macaques with gp120 (for week 8 versus week 11, $P = 0.0002$ and $P < 0.0001$ for vaccinated and unvaccinated groups, respectively) (Fig. 7A). Upon release from ART, the PC/PB numbers declined and reached values similar to those seen prior to ART.

These changes were mirrored by the enumeration of SIV Env-specific B-cell ELISpots in bone marrow (Fig. 8A). Over the first 8 weeks of ART, numbers of B-cell ELISpots declined significantly in all groups combined ($P = 0.019$) but were subsequently increased in the unvaccinated and vaccinated boosted groups by week 11. The increases in the two boosted groups were significantly different from the unboosted controls ($P = 0.019$). Upon the cessation of ART, PC/PB stabilized at levels similar to those seen prior to ART.

In PBMC, no significant changes in PC/PB were seen over the first 8 weeks of ART (Fig. 7B). An increase in numbers of PC/PB was observed between weeks 8 and 11 for both the vaccinated and unvaccinated macaques ($P < 0.0001$ for both), reflecting the protein boost. The controls also exhibited a slight increase in PC/PB

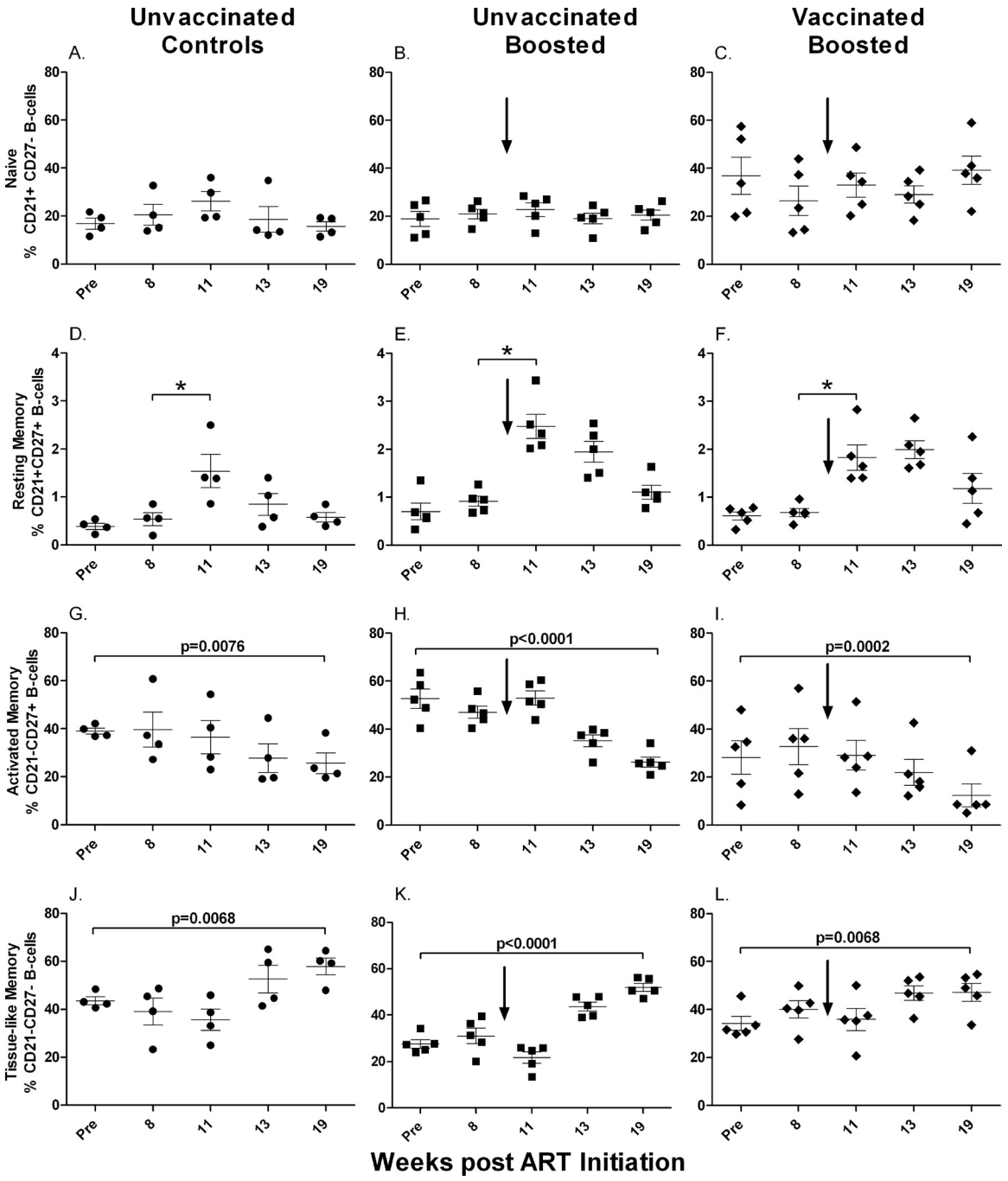


**FIG 4** Memory B cells in PBMC over the course of the study. Changes in naïve (A to C), resting memory (D to F), activated memory (G to I), and tissue-like memory (J to L) B cells are shown. *, differences between week 8 and week 11 values, normalized to pre-ART values, were significantly elevated ($P < 0.0001$ for each group). Values for individual animals are plotted, with the group means (long solid lines) and standard errors of the means (short solid lines) shown. Arrows indicate boosting with SIV gp120 at week 9.

levels between weeks 8 and 11 ($P = 0.0037$), likely due to ART. However, at week 11, levels in both boosted groups were significantly elevated over those of the controls ($P = 0.0019$ and 0.0011 for the unvaccinated and vaccinated groups, respectively). Upon release from ART, PC/PB levels declined; however, the unvaccinated and vaccinated macaques retained elevated values compared to those of the controls at week 13 ($P = 0.014$ for both) and at week 19 ($P = 0.045$ and 0.0077 for the unvaccinated and vaccinated groups, respectively). Overall, the unvaccinated boosted macaques exhibited elevated PC/PB levels at week 19 compared to pre-ART levels ($P = 0.029$).

Similar to the results obtained with bone marrow cells, SIV Env-specific B-cell ELISpot data for PBMC (Fig. 8B) mirrored the pattern of PC/PB levels in blood. Taking all macaques together, an overall decline in numbers of ELISpots resulted from the first 8 weeks of ART. Subsequently, upon the boosting of the unvacci-

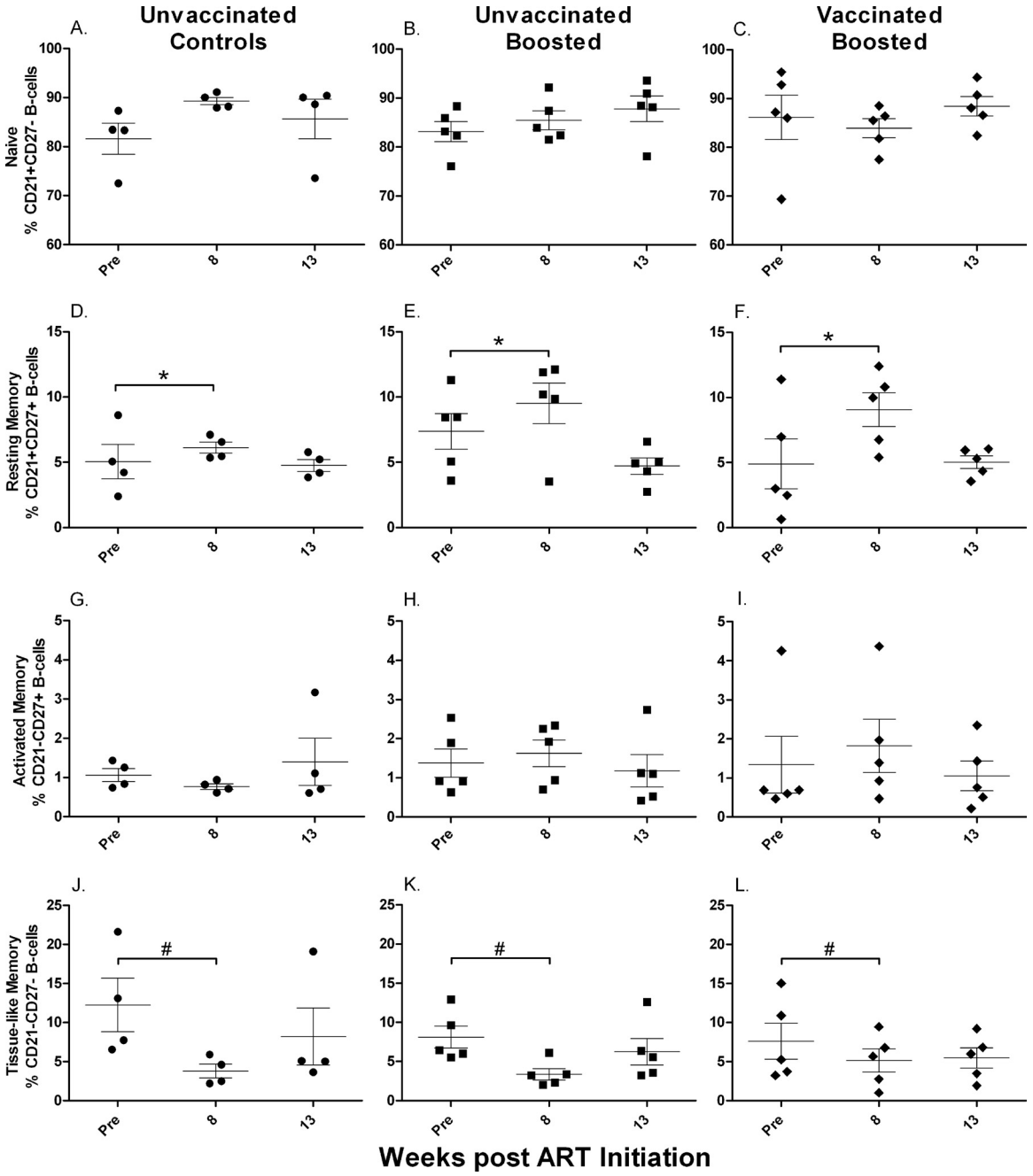


**FIG 5** Memory B cells in lymph node over the course of the study. Changes in naïve (A to C), resting memory (D to F), activated memory (G to I), and tissue-like memory (J to L) B cells are shown. *, significant increase in numbers of resting memory B cells when all groups were combined ($P = 0.0034$); #, significant decrease in numbers of tissue-like memory B cells when all groups were combined ($P = 0.0029$). Values for individual animals are plotted, with the group means (long solid lines) and standard errors of the means (short solid lines) shown.

nated and vaccinated groups with gp120, elevated numbers of ELISpots were seen in both groups, significantly different from the unboosted controls ($P = 0.026$). As in bone marrow, no differences between the unvaccinated and vaccinated groups were observed. Overall, however, by week 19 of the study, ELISpot levels were similar to those seen prior to ART.

The protein boost exhibited no measurable effect on the PC/PB population in lymph nodes of any of the groups. Overall PC/PB levels remained stable throughout the study (data not shown).

**Serum anti-SIV gp120 titers show independence from bone marrow and PBMC memory B cells measured by an ELISpot assay.** Although we saw differences in B-cell ELISpot responses associated with envelope protein boosting, IgG Env-specific binding titers remained stable over the course of the study in the unvaccinated and vaccinated macaques (Fig. 8C). During ART, titers modestly but nonsignificantly declined in the control group but rebounded with increasing viremia upon release from ART. By week 19, titers in all groups were not different from pre-ART levels.

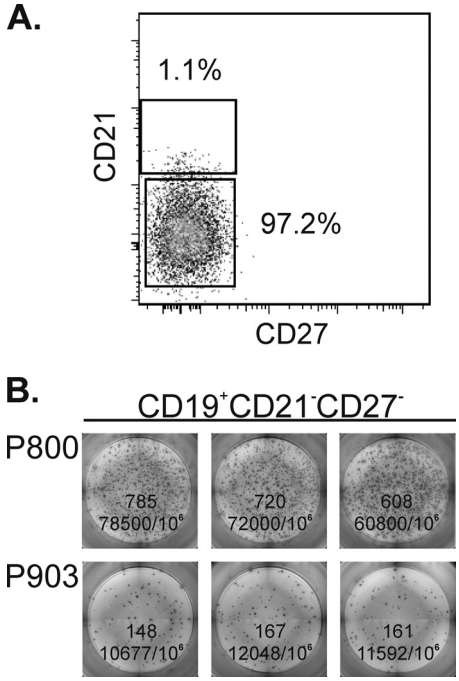


**FIG 6** Spontaneous secretion of antibody by sorted CD21$^-$/CD27$^-$ bone marrow B cells. (A) Representative purity of sorted, cryopreserved bone marrow cells from macaque P800. (B) Representative B-cell IgG ASC for 2 of the 4 macaque bone marrow samples sorted following overnight incubation with no stimulation. Triplicate wells are shown for each sample, with the number of ELISpots per well and the calculated number of ASC/$10^6$ sorted cells indicated.

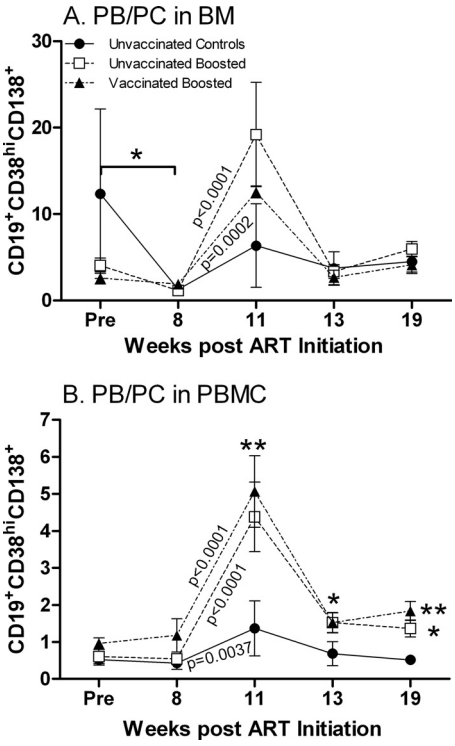


**FIG 7** PC/PB dynamics in BM and PBMC during the study. (A) PB/PC in bone marrow. *, significant decrease in numbers of PC/PB in all groups combined over 8 weeks of ART ($P = 0.011$). (B) PB/PC in PBMC. A significant difference between unvaccinated and vaccinated boosted groups compared to controls was observed at week 11 (**, $P = 0.0019$ and $P = 0.0011$, respectively), week 13 (*, $P = 0.014$ for both), and week 19 (*, $P = 0.045$ for the unvaccinated boosted group compared to controls; **, $P = 0.0077$ for the vaccinated boosted group compared to controls). The unvaccinated boosted group exhibited elevated PC/PB levels at week 19 compared to pre-ART levels ($P = 0.029$). Plotted are the group means ± standard errors of the means.

**Loss of activated memory B cells is not due to enhanced exhaustion, as measured by PD-1 expression.** In view of the decline in the activated memory B-cell population in blood (Fig. 4G to I) and the downward trend in bone marrow (Fig. 3H and I) over the 19 weeks of the study, we investigated whether this was due to an increased exhaustion associated with PD-1 expression, as was reported previously for both T cells (9, 26) and B cells (58). The majority of activated memory B cells in healthy rhesus monkeys express PD-1 (58). Therefore, instead of reporting changes in percentages, we examined changes in MFI. In bone marrow, the PD-1 expression level was elevated in both the unvaccinated boosted and vaccinated boosted macaques over the first 8 weeks of ART ($P = 0.0007$ and $P < 0.0001$, respectively) and also following the protein boost (for week 11 versus pre-ART levels, $P = 0.0089$ and $P = 0.0005$, respectively) (Fig. 9A). The cause of the initial increase is not known, but the elevated expression level of PD-1 was likely sustained by the activation of the B cells by the protein booster immunization. By week 19, the MFI of PD-1 on macaque activated memory cells in all groups was restored to pre-ART levels. In PBMC, mean PD-1 MFI levels similarly increased in the unvaccinated and vaccinated groups by week 11 ($P = 0.028$ and $P = 0.0070$, respectively). However, by week 19, levels in all groups combined were significantly lower than pre-ART levels ($P = 0.029$) (Fig. 9B). Overall, the decline in levels of activated memory B cells in blood and bone marrow could not be attributed to increased PD-1 expression levels.

**Expression of CD22.** We further examined the expression on activated memory B cells of CD22 (SIGLEC-2 [sialic acid binding immunoglobulin-like lectin receptor]), which is expressed on all B cells (a pan-B-cell marker in humans), including activated and memory B cells. SIGLEC-2 binds to α2-6-linked sialic acid and can colocalize with the B-cell receptor to inhibit B-cell activation (42, 44). It is lost upon plasma cell differentiation (42). Not only is CD22 an inhibitory receptor for B cells, it also plays a role in bone marrow homing of mature, recirculating B cells in mice (42). Here, in bone marrow, the percentage of CD22-positive cells exhibited an upward trend over the first 8 weeks of ART in all groups (Fig. 9C) but subsequently began to decline following the Env boost and release from ART. Thus, the unvaccinated and vaccinated groups showed reductions for the latter 3 time points between weeks 8 and 19. Only the vaccinated boosted group had a significant downward slope (−3.4%/day; $P = 0.0021$). The changes in the three groups were not different from one another. Moreover, over the entire treatment regimen, there was not a significant difference in CD22 expression levels between week 19 and pre-ART values for any macaque group.

CD22-expressing activated memory B cells showed a different pattern in PBMC (Fig. 9D). The control group exhibited essentially unchanged values, whereas the two vaccinated groups showed significantly reduced expression levels of CD22 over the entire course of the regimen, with significant negative slopes of −1.2% and −2.1%/day for the unvaccinated and vaccinated groups, respectively ($P = 0.017$ and $P < 0.0001$, respectively). The

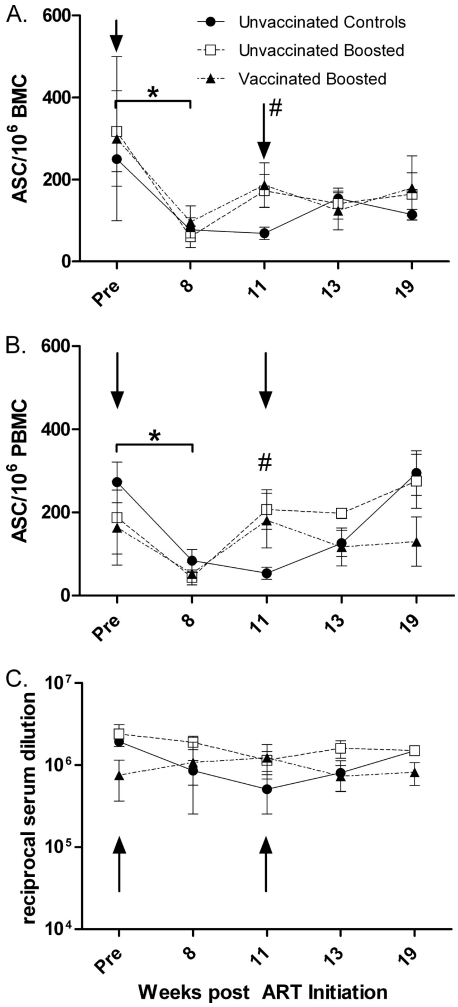


**FIG 8** Frequency of ASC in BM and PBMC, and anti-gp120 binding titers in serum over the course of the study. (A and B) Env-specific IgG-secreting B cells in BM (A) and PBMC (B). *, significant decreases in numbers of ASC when all groups were combined ($P = 0.019$ for bone marrow; $P = 0.0018$ for PBMC); #, values for unvaccinated and vaccinated boosted groups were significantly elevated compared to the values for the controls at week 11 ($P = 0.019$ for bone marrow; $P = 0.026$ for PBMC). (C) Serum binding titers against SIVmac251 gp120. Plotted are the group means ± standard errors of the means. Arrows indicate times of ART treatment (0 to 11 weeks).

slopes of the unvaccinated and vaccinated groups were not different from one another. Moreover, the decreases in the CD22 expression levels at week 19 compared to the pre-ART values were significantly different for the two boosted groups ($P = 0.015$ and $P < 0.0001$ for the unvaccinated and vaccinated groups, respectively). These changes are consistent with the increases in the numbers of PC/PB in both boosted groups at week 19 compared to the controls (Fig. 7B) and with the increase in numbers of PC/PB in the unvaccinated boosted group at week 19 compared to the pre-ART level.

## DISCUSSION

In this study, we found no benefit of ART for chronically SIV-infected macaques, with regard to lasting decreases in plasma viremia and increases in $CD4^+$ T-cell counts, and no improved outcome following therapeutic SIV envelope boosting, regardless of the prior vaccination status. Although the ART regimen decreased viremia approximately 2 logs within the first 2 weeks of treatment, as expected (61) (Fig. 1A), further decreases occurred by chance only in the control macaque group. Greater viremia control might have resulted if treatment had been prolonged or initiated earlier (2), but here we used available macaques, recycled from other studies, that had been infected for 27 to 65 weeks. The use of a combination HAART regimen incorporating protease and integrase inhibitors in addition to reverse transcriptase inhibitors might also have improved viremia control and the overall outcome (13).

In spite of the late initiation of ART, numerous changes seen in both PC/PB populations and levels of ASC in response to boosting with gp120 over the course of treatment suggested that the approach taken might be of benefit if the ART regimen was continued for a longer period of time and/or initiated earlier following SIV infection or if a more robust vaccine regimen had been used. In both boosted groups, these changes included significant increases in Env-specific ASC (Fig. 8A and B) and PC/PB (Fig. 7A and B) in both PBMC and bone marrow. Overall, the transient increases in ASC and PC/PB demonstrated the ability of B cells in chronically infected macaques to respond to an antigenic stimulus. The MPL-SE adjuvant was also likely a contributing factor. MPL is a Toll-like receptor 4 (TLR4) agonist derived from *Salmonella enterica* serovar Minnesota, and it induces strong Th1 and IL-12 responses (16). Tonsillar memory and naïve B cells do not express TLR4; however, PC do (14). Their expansion seen here may be due in part to the TLR4-containing adjuvant. This question can be resolved in future studies by staining antienvelope-specific as well as total memory B cells.

The identification of $CD27^-$ PC/PB deserves comment, as human PC/PB have been defined as $CD27^+$ (5). We demonstrated that sorted $CD21^-$ $CD27^-$ B cells spontaneously secrete IgG and IgA (Fig. 8A and B), confirming that these cells are PC/PB. However, whether this $CD27^-$ PC/PB macaque B-cell population is induced by SIV infection and manifested during chronic infection or naturally occurs in healthy monkeys, not studied here, needs to be further explored. HIV infection leads to impaired B-cell and antibody responses (39). Among these responses are increases in numbers of tissue-like memory ($CD21^-$ $CD27^-$) B cells, which exhibit features of premature exhaustion and display elevated levels of HIV-specific ASC following short-term stimulation compared to the levels in classical memory cells. A similar B-cell dysfunction occurs in hepatitis C virus infection, another persistent viral infection, where CD27 is downregulated on memory B ASC, an effect most likely resulting from bystander T-cell help without specific antigen stimulation of the B-cell receptor, leading to short-term antibody secretion and eventual apoptosis (47). In both of those reports, however, the cells were not identified as PC/PB, as the spontaneous secretion of antibody was not assessed. Alternatively, rather than a manifestation of immune dysfunction, $CD27^-$ PC/PB may arise by a simple shedding process. Activated T, NK, and B cells all express cell surface CD27 (63), which can be proteolytically cleaved to produce a soluble form (sCD27). sCD27 levels are elevated in HIV-infected individuals (1, 12, 48) and correlate with plasma viremia (12) but can be decreased by successful HAART treatment over time. Further studies will be needed to determine the prevalence of $CD27^-$ and $CD27^+$ PC/PB in healthy and immunodeficient hosts and whether they exhibit functional differences. To this end, as CD138 can be expressed on pre-B cells

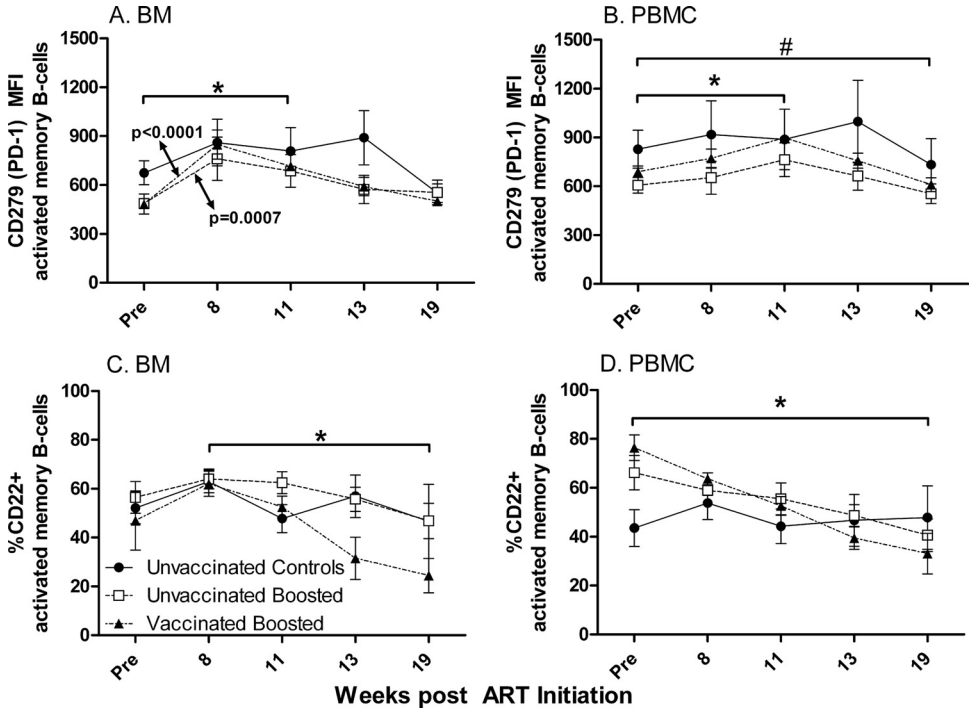


**FIG 9** CD279 (PD-1) and CD22 levels on activated memory B cells in BM and PBMC during the study. (A) Mean fluorescence intensity (MFI) of PD-1 on BM activated memory B cells. *, significant increase in expression levels over 11 weeks of ART ($P = 0.0089$ for unvaccinated boosted macaques; $P = 0.0005$ for vaccinated boosted macaques). (B) MFI of PD-1 on PBMC activated memory B cells. *, significant increase in expression levels over 11 weeks of ART ($P = 0.028$ for unvaccinated boosted macaques; $P = 0.0070$ for vaccinated boosted macaques); #, decline in PD-1 MFI at week 19 compared to pre-ART values for all groups combined ($P = 0.029$). (C) CD22 expression on activated memory B cells in bone marrow. *, significant negative slope of the vaccinated boosted macaque group over weeks 8 to 19 ($P = 0.0021$). (D) CD22 expression on activated memory B cells in PBMC. *, significant negative slopes of unvaccinated boosted and vaccinated boosted macaque groups from pre-ART values to week 19 ($P = 0.017$ and $P < 0.0001$, respectively). Plotted are group means ± standard errors of the means.

as well as PC/PB (31), additional markers, such as Ki67 or IgD, should be used in future studies for the routine phenotyping of macaque PC/PB.

Memory B-cell subpopulations have been described previously for SIV-infected and uninfected rhesus macaques (8, 28, 58), SIV-infected sooty mangabeys (58), and SIV- or simian-human immunodeficiency virus (SHIV)-infected and uninfected cynomolgus monkeys (27, 46, 62). The B-cell subpopulations studied here, defined as either naïve or resting, activated, or tissue-like memory, are similar to those reported previously for SIV- and SHIV-infected animals (27, 58). Over the course of the study, we observed significant changes in individual populations, predominantly in PBMC, with fewer changes in bone marrow and even fewer in lymph node. In PBMC, transient increases in the minor population of resting memory B cells were observed during ART for all macaque groups (Fig. 4D to F). However, prolonged changes were seen in the two other B-cell memory populations. Levels of activated memory B cells decreased in all macaque groups over the 19-week regimen (Fig. 4G to I). A similar decline in the number of activated memory B cells in PBMC during ART was previously described for both humans and monkeys (6, 27, 46). Here the decline continued upon the release from ART despite therapeutic gp120 boosting. At the same time, tissue-like memory B-cell patterns over the course of treatment began to change upon the release from ART and viral rebound, resulting in an overall elevated level over the course of the study (Fig. 4J to L). Tissue-like memory B cells were originally described as a unique subpopulation of memory B cells in human tonsillar tissue which expressed an inhibitory receptor, Fc receptor homologue 4 (17). As mentioned above, although they exhibit enriched HIV-specific responses in infected humans, they have been characterized as exhausted and were suggested to contribute to the poor antibody responses seen with HIV infection (39). Therefore, the increase in their levels here may reflect dysfunctional B cells and may explain the lack of increased serum antibody levels in the Env-boosted macaques (Fig. 8C).

Factors affecting the significant decline in numbers of activated memory B cells from PMBC over the course of the treatment are not known. One possibility is increased trafficking to lymphoid organs (46). Here we did not specifically address B-cell homing or trafficking but saw no change in the activated memory population in the lymph node samples. However, we did not examine B-cell subpopulations in spleen or gut mucosal tissue. Viral proteins, reported to play a role in B-cell dysfunction, may also have contributed to the loss of activated memory B cells. Here abundant viral proteins should have been expressed as a result of the suboptimal ART regimen, which poorly suppressed viremia, particularly in the two boosted groups (Fig. 2A). These two groups in fact exhibited a trend toward a loss of activated memory B cells in bone marrow (Fig. 3H and I). In addition, significantly decreased levels of activated memory B cells were observed in PBMC of all three macaque groups (Fig. 4G to I). The viral Nef protein was shown previously to suppress B-cell IgA and IgG2 responses and to contribute to the dysfunction of B cells (38, 56, 65). In addition, Tat is

able to upregulate CD95 (Fas) on B cells in HIV and SIV infections (6, 20, 27, 28, 53, 57), which might prime these cells toward apoptosis (40). However, memory B cells ordinarily express CD95 to a high degree (28), as confirmed by our own unpublished studies, where over 70% of $CD27^+$ $CD20^+$ B cells from healthy macaques expressed CD95. Therefore, enhanced CD95-mediated apoptosis cannot be the sole reason for the continued decline in levels of memory B cells over the course of our study.

For SIV-infected rhesus macaques that become rapid progressors, PD-1 has been shown to play a role in the rapid depletion of activated memory B cells within 2 weeks of infection, whereas in typical progressors, the initial loss of memory B cells is transient (58). Here we found no association between the continued loss of activated memory B cells in the chronically infected macaques and PD-1 expression. The PD-1 ligand PD-L1 (B7-H1) has been shown to be upregulated in both HIV infection (50) and SIV infection (66) and may be a critical factor in T-cell anergy and survival. Whether it plays a role in the control of B cells is not known, but it would be of interest to pursue this question in future studies.

The CD22 expression level on activated memory B cells in PBMC of the unvaccinated and vaccinated boosted groups exhibited an overall decline, extending from the pre-ART time point to week 19 (Fig. 9D). Over the same interval, at least the unvaccinated boosted group displayed a modestly elevated level of PC/PB, consistent with the known loss of CD22 expression on plasma cells. However, whether CD22 could contribute to the loss of activated memory B cells in HIV and SIV infections is not known. Previous studies using intravenous immunoglobulin, which is able to bind CD22 by means of its sialic acid component, have shown that the cross-linking of CD22 together with the activation of the B-cell receptor by bound antigen or antibody can induce B-cell apoptosis (52). Whether altered glycosylation patterns arising in HIV or SIV infection might result in such an operative mechanism and contribute to the elimination of activated memory B cells requires further investigation.

Finally, the decline in levels of $CD21^-$ $CD27^+$ activated memory B cells might be due in part to the shedding of the receptor, as discussed above. CD27 shedding would reduce the subpopulation of $CD21^-$ $CD27^+$ activated memory B cells, potentially increasing the $CD21^-$ $CD27^-$ subpopulation of tissue-like memory B cells. Indeed, significant changes in these PBMC subpopulations were observed (Fig. 4G to L). Furthermore, an increase in the number of cells with the phenotype of tissue-like memory B cells was previously reported for HIV-infected patients (39), supporting our results.

Here we confirmed the findings reported previously by Morris et al. (41) showing that SIV-specific ASC counts in PBMC decline during ART (Fig. 8B) but extended this observation by showing that this also occurs in bone marrow (Fig. 8A). Although we subsequently saw an expansion of SIV Env-specific ASC in bone marrow and PBMC after boosting in the unvaccinated and vaccinated macaque groups (Fig. 8A and B), the higher levels were not sustained postboosting despite rebounding viremia, nor did they reach levels higher than those seen prior to ART. This pattern is similar to that of an early ASC response, which occurs in extrafollicular foci and expands and contracts rapidly (60). Long-lived ASC develop in germinal centers and ultimately result in plasma cells that migrate to the bone marrow. As we saw no lasting increase in PC/PB counts in the bone marrow and no overall changes in lymph node memory B cells, we interpret this result as reflecting germinal center loss or dysfunction in the chronically infected macaques. It is known that germinal centers are damaged and reduced in size and number during HIV and SIV infections (33, 35). Thus, although B cells were able to respond to the protein boost, long-term B-cell memory did not develop.

In spite of the continued loss of activated memory B cells from PBMC and bone marrow, serum titers against SIV gp120 remained constant (Fig. 8C). This disconnect between memory B cells and titers has been described for HIV-infected patients for antibodies to pneumococcal antigens (15) and to HIV antigens (30) and in SIV-infected animals (28). Here it reflects the continuous presence of long-lived PC/PB in both bone marrow and PBMC compartments (Fig. 7A and B) established prior to B-cell dysfunction.

In summary, no improvement in the control of viremia and preservation of CD4 cells resulted from therapeutic vaccination after animals were released from ART. Numbers of activated memory B cells continued to decline in both PBMC and bone marrow. This decline was not reversed by boosting with SIV envelope protein, although B cells were still responsive, as evidenced by the transient increases in levels of Env-specific ASC. Furthermore, PC/PB in PBMC and bone marrow were expanded, and PBMC exhibited a persistent small increase in PC/PB levels at the end of the study regimen. Future studies should explore the time frame in which an effective boosting regimen in conjunction with ART could significantly enhance antiviral humoral immunity, potentially contributing to reduced viremia and slower disease progression. Defining, for example, the $CD4^+$ T-cell threshold below which therapeutic protein boosting is ineffective could significantly improve treatment regimens.

## ACKNOWLEDGMENTS

We thank Deborah Weiss, James Treece, and the staff at Advanced BioScience Laboratories, Inc., for all animal care and procedures; Genoveffa Franchini for providing the recycled macaques; Ian Morgan for technical help; and L. Jean Patterson for critical reading of the manuscript. The following reagent was obtained through the AIDS Research and Reference Reagent Program, Division of AIDS, NIAID, NIH: CEM.$NK^R$, from Peter Cresswell.

This work was supported by the Intramural Research Program of the National Institutes of Health National Cancer Institute.

## REFERENCES

1. **Atlas A, et al.** 2004. Effects of potent antiretroviral therapy on the immune activation marker soluble CD27 in patients infected with HIV-1 subtypes A-D. J. Med. Virol. **72**:345–351.
2. **Boasso A, et al.** 2009. Combined effect of antiretroviral therapy and blockade of IDO in SIV-infected rhesus macaques. J. Immunol. **182**:4313–4320.
3. **Brocca-Cofano E, et al.** 2011. Vaccine-elicited SIV and HIV envelope-specific IgA and IgG memory B cells in rhesus macaque peripheral blood correlate with functional antibody responses and reduced viremia. Vaccine **29**:3310–3319.
4. **Cagigi A, Nilsson A, Pensieroso S, Chiodi F.** 2010. Dysfunctional B-cell responses during HIV-1 infection: implication for influenza vaccination and highly active antiretroviral therapy. Lancet Infect. Dis. **10**:499–503.
5. **Cannizzo E, et al.** 2010. Multiparameter immunophenotyping by flow cytometry in multiple myeloma: the diagnostic utility of defining ranges of normal antigenic expression in comparison to histology. Cytometry B Clin. Cytom. **788**:231–238.
6. **Chong Y, et al.** 2004. Selective CD27+ (memory) B cell reduction and characteristic B cell alteration in drug-naive and HAART-treated HIV type 1-infected patients. AIDS Res. Hum. Retroviruses **20**:219–226.
7. **Cohen MS, et al.** 2011. Prevention of HIV-1 infection with early antiretroviral therapy. N. Engl. J. Med. **365**:493–505.

8. **Das A, et al.** 2011. Double-positive CD21+CD27+ B cells are highly proliferating memory cells and their distribution differs in mucosal and peripheral tissues. PLoS One **6**:e16524. doi:10.1371/journal.pone.0016524.
9. **Day CL, et al.** 2006. PD-1 expression on HIV-specific T cells is associated with T-cell exhaustion and disease progression. Nature **443**:350–354.
10. **Demberg T, et al.** 2008. Sequential priming with simian immunodeficiency virus (SIV) DNA vaccines, with or without encoded cytokines, and a replicating adenovirus-SIV recombinant followed by protein boosting does not control a pathogenic SIVmac251 mucosal challenge. J. Virol. **82**:10911–10921.
11. **De Milito A.** 2004. B lymphocyte dysfunctions in HIV infection. Curr. HIV Res. **2**:11–21.
12. **De Milito A, et al.** 2002. Plasma levels of soluble CD27: a simple marker to monitor immune activation during potent antiretroviral therapy in HIV-1-infected subjects. Clin. Exp. Immunol. **127**:486–494.
13. **Dinoso JB, et al.** 2009. A simian immunodeficiency virus-infected macaque model to study viral reservoirs that persist during highly active antiretroviral therapy. J. Virol. **83**:9247–9257.
14. **Dorner M, et al.** 2009. Plasma cell Toll-like receptor (TLR) expression differs from that of B cells, and plasma cell TLR triggering enhances immunoglobulin production. Immunology **128**:573–579.
15. **D'Orsogna LJ, Krueger RG, McKinnon EJ, French MA.** 2007. Circulating memory B-cell subpopulations are affected differently by HIV infection and antiretroviral therapy. AIDS **21**:1747–1752.
16. **Duthie MS, Windish HP, Fox CB, Reed SG.** 2011. Use of defined TLR ligands as adjuvants within human vaccines. Immunol. Rev. **239**:178–196.
17. **Ehrhardt GRA, et al.** 2005. Expression of the immunoregulatory molecule FcRH4 defines a distinctive tissue-based population of memory B cells. J. Exp. Med. **202**:783–791.
18. **Fogli M, et al.** 5 March 2012. Emergence of exhausted B cells in asymptomatic HIV-1-infected patients naïve for HAART is related to reduced immune surveillance. Clin. Dev. Immunol. doi:10.1155/2012/829584.
19. **Gudmundsdotter L, et al.** 2008. Long-term increase of CD4+ central memory cells in HIV-1-infected individuals by therapeutic HIV-1 rgp160 immunization. Vaccine **26**:5107–5110.
20. **Haas A, Zimmermann K, Oxenius A.** 2011. Antigen-dependent and -independent mechanisms of T and B cell hyperactivation during chronic HIV-1 infection. J. Virol. **85**:12102–12113.
21. **Halwani R, et al.** 2008. Therapeutic vaccination with simian immunodeficiency virus (SIV)-DNA + IL-12 or IL-15 induces distinct CD8 memory subsets in SIV-infected macaques. J. Immunol. **180**:7969–7979.
22. **Ho J, et al.** 2006. Two overrepresented B cell populations in HIV-infected individuals undergo apoptosis by different mechanisms. Proc. Natl. Acad. Sci. U. S. A. **103**:19436–19441.
23. **Howell DN, Andreotti JR, Cresswell P.** 1985. Natural killing target antigens as inducers of interferon; studies with an immunoselected, natural-killing-resistant human T-lymphoblastoid cell line. J. Immunol. **134**: 971–976.
24. **Hu H, et al.** 2011. SIV antigen immunization induces transient antigen-specific T cell responses and selectively activates viral replication in draining lymph nodes in retroviral suppressed rhesus macaques. Retrovirology **8**:57. doi:10.1186/1742-4690-8-57.
25. **Jin X, et al.** 2002. Safety and immunogenicity of ALVAC vCP1452 and recombinant gp160 in newly human immunodeficiency virus type 1-infected patients treated with prolonged highly active antiretroviral therapy. J. Virol. **76**:2206–2216.
26. **Kaufmann DE, Walker BD.** 2008. Programmed death-1 as a factor in immune exhaustion and activation in HIV infection. Curr. Opin. HIV AIDS **3**:362–367.
27. **Kling HM, Shipley TW, Norris KA.** 2011. Alterations in peripheral blood B-cell populations in SHIV89.6P-infected macaques (Macacca fascicularis). Comp. Med. **61**:269–277.
28. **Kuhrt D, et al.** 2010. Evidence of early B-cell dysregulation in simian immunodeficiency virus infection: rapid depletion of naive and memory B-cell subsets with delayed reconstitution of the naive B-cell population. J. Virol. **84**:2466–2476.
29. **Kundu-Raychaudhuri S, et al.** 2001. Effect of therapeutic immunization with HIV type 1 recombinant glycoprotein 160 ImmunoAG vaccine in HIV-infected individuals with CD4+ T cell counts of > or =500 and 200–400/mm3 (AIDS Clinical Trials Group Study 246/946). AIDS Res. Hum. Retroviruses **17**:1371–1378.
30. **Kunz K, et al.** 2011. A broad spectrum of functional HIV-specific memory B cells in the blood of infected individuals with high CD4+ T-cell counts. J. Acquir. Immune Defic. Syndr. **57**:e56–e58. doi:10.1097/QAI/06013e31821dd9d1.
31. **Kyrtsonis M, et al.** 2011. CD138 expression helps distinguishing Waldnstrom's macroglobulinemia (WM) from splenic marginal zone lymphoma (SMZL). Clin. Lymphoma Myeloma Leuk. **11**:99–102.
32. **Lee EM, et al.** 2010. Molecular methods for evaluation of virological status of nonhuman primates challenged with simian immunodeficiency or simian-human immunodeficiency viruses. J. Virol. Methods **163**:287–294.
33. **Levesque MC, et al.** 2009. Polyclonal B cell differentiation and loss of gastrointestinal tract germinal centers in the earliest stages of HIV-1 infection. PLoS Med. **6**:e1000107. doi:10.1371/journal.pmed.1000107.
34. **Malaspina A, et al.** 2006. Appearance of immature/transitional B cells in HIV-infected individuals with advanced disease: correlation with increased IL-7. Proc. Natl. Acad. Sci. U. S. A. **103**:2262–2267.
35. **Margolin DH, et al.** 2006. Germinal center function in the spleen during simian HIV infection in rhesus monkeys. J. Immunol. **177**:1108–1119.
36. **Medina F, Segundo C, Campos-Caro A, Gonzalez-Garcia I, Brieva JA.** 2002. The heterogeneity shown by human plasma cells from tonsil, blood, and bone marrow reveals graded stages of increasing maturity, but local profiles of adhesion molecule expression. Blood **99**:2154–2161.
37. **Moir S, et al.** 2010. B cells in early and chronic HIV infection: evidence for preservation of immune function associated with early initiation of antiretroviral therapy. Blood **116**:5571–5579.
38. **Moir S, Fauci AS.** 2010. Nef, macrophages and B cells: a highway for evasion. Immunol. Cell Biol. **88**:1–2.
39. **Moir S, et al.** 2008. Evidence for HIV-associated B cell exhaustion in a dysfunctional memory B cell compartment in HIV-infected viremic individuals. J. Exp. Med. **205**:1797–1805.
40. **Moir S, et al.** 2004. Decreased survival of B cells of HIV-viremic patients mediated by altered expression of receptors of the TNF superfamily. J. Exp. Med. **200**:587–599.
41. **Morris L, et al.** 1998. HIV-1 antigen-specific and -nonspecific B cell responses are sensitive to combination antiretroviral therapy. J. Exp. Med. **188**:233–245.
42. **Nitschke L.** 2009. CD22 and Siglec-G: B-cell inhibitory receptors with distinct functions. Immunol. Rev. **230**:128–143.
43. **Notermans DW, et al.** 2001. Potent antiretroviral therapy initiates normalization of hypergammaglobulinemia and a decline in HIV type 1-specific antibody responses. AIDS Res. Hum. Retroviruses **17**:1003–1008.
44. **O'Reilly MK, Tian H, Paulson JC.** 2011. CD22 is a recycling receptor that can shuttle cargo between the cell surface and endosomal compartments of B cells. J. Immunol. **186**:1554–1563.
45. **Perez-Andres M, et al.** 2010. Human peripheral blood B-cell compartments: a crossroad in B-cell traffic. Cytometry B Clin. Cytom. **78**(Suppl 1):S47–S60. doi:10.1002/cyto.b.20547.
46. **Peruchon S, et al.** 2009. Tissue-specific B-cell dysfunction and generalized memory B-cell loss during acute SIV infection. PLoS One **4**:e5966. doi:10.1371/journal.pone.0005966.
47. **Racanelli V, et al.** 2006. Antibody production and in vitro behavior of CD27-defined B-cell subsets: persistent hepatitis C virus infection changes the rules. J. Virol. **80**:3923–3934.
48. **Regidor DL, et al.** 2011. Effect of highly active antiretroviral therapy on biomarkers of B-lymphocyte activation and inflammation. AIDS **25**:303–314.
49. **Romano JW, et al.** 2000. Quantitative evaluation of simian immunodeficiency virus infection using NASBA technology. J. Virol. Methods **86**:61–70.
50. **Rosignoli G, et al.** 2007. Expression of PD-L1, a marker of disease status, is not reduced by HAART in aviraemic patients. AIDS **21**:1379–1381.
51. **Rossi MID, et al.** 2003. B lymphopoiesis is active throughout human life, but there are developmental age-related changes. Blood **101**:576–584.
52. **Seite JF, et al.** 2010. IVIg modulates BCR signaling through CD22 and promotes apoptosis in mature human B lymphocytes. Blood **116**:1698–1704.
53. **Shen X, Tomaras GD.** 2011. Alterations of the B-cell response by HIV-1 replication. Curr. HIV/AIDS Rep. **8**:23–30.
54. **Shimada M, et al.** 2009. Effect of therapeutic immunization using Ad5/35 and MVA vectors on SIV infection of rhesus monkeys undergoing antiretroviral therapy. Gene Ther. **16**:218–228.
55. **Silva R, et al.** 2011. CD300a is expressed on human B cells, modulates BCR-mediated signaling, and its expression is down-regulated in HIV infection. Blood **117**:5870–5880.

56. **Swingler S, et al.** 2008. Evidence for a pathogenic determinant in HIV-1 Nef involved in B cell dysfunction in HIV/AIDS. Cell Host Microbe **4**:63–76.
57. **Titanji K, et al.** 2005. Primary HIV-1 infection sets the stage for important B lymphocyte dysfunctions. AIDS **19**:1947–1955.
58. **Titanji K, et al.** 2010. Acute depletion of activated memory B cells involves the PD-1 pathway in rapidly progressing SIV-infected macaques. J. Clin. Invest. **120**:3878–3890.
59. **Verhoeven D, Sankaran S, Silvey M, Dandekar S.** 2008. Antiviral therapy during primary simian immunodeficiency virus infection fails to prevent acute loss of CD4 T cells in gut mucosa but enhances their rapid restoration through central memory T cells. J. Virol. **82**:4016–4027.
60. **Vikstrom I, Tarlinton DM.** 2011. B cell memory and the role of apoptosis in its formation. Mol. Immunol. **48**:1301–1306.
61. **von Gegerfelt AS, et al.** 2007. Long-lasting decrease in viremia in macaques chronically infected with simian immunodeficiency virus SIVmac251 after therapeutic DNA immunization. J. Virol. **81**:1972–1979.
62. **Vugmeyster Y, et al.** 2004. B-cell subsets in blood and lymphoid organs in Macaca fascicularis. Cytometry A **61**:69–75.
63. **Widney D, et al.** 1999. Aberrant expression of CD27 and soluble CD27 (sCD27) in HIV infection and in AIDS-associated lymphoma. Clin. Immunol. **93**:114–123.
64. **Xiao P, et al.** 2012. Replicating adenovirus-simian immunodeficiency virus (SIV) recombinant priming and envelope protein boosting elicits localized, mucosal IgA immunity in rhesus macaques correlated with delayed acquisition following a repeated low-dose rectal SIVmac251 challenge. J. Virol. **86**:4644–4657.
65. **Xu W, et al.** 2009. HIV-1 evades virus-specific IgG2 and IgA responses by targeting systemic and intestinal B cells via long-range intercellular conduits. Nat. Immunol. **10**:1008–1017.
66. **Xu H, et al.** 2010. Increased B7-H1 expression on dendritic cells correlates with programmed death 1 expression on T cells in simian immunodeficiency virus-infected macaques and may contribute to T cell dysfunction and disease progression. J. Immunol. **185**:7340–7348.